

## Glass-ionomer Cement SiO<sub>2</sub>, Al<sub>2</sub>O<sub>3</sub>, Na<sub>2</sub>O, CaO, P<sub>2</sub>O<sub>5</sub>, F<sup>-</sup> Containing Alternative Additive of Zn and Sr Prepared by Sol–gel method

**KH. M. Tohamy, N. Abd El Sameca<sup>\*</sup>, T.M. Tiama<sup>\*\*</sup> and I. Soliman<sup>\*\*</sup>**

*Physics Department, Faculty of Science, Al-Azhar University, Nasr City, Cairo; <sup>\*\*</sup>Dental Material Department, Faculty of Dentistry, and <sup>\*\*</sup>Knowledge Center, Faculty of Pharmacy, Misr University for Science & Technology, 6<sup>th</sup> Oct. City, Egypt.*

**G**lass-Ionomer cement with composition SiO<sub>2</sub>, Al<sub>2</sub>O<sub>3</sub>, Na<sub>2</sub>O, CaO, P<sub>2</sub>O<sub>5</sub>, F<sup>-</sup> with substitute ZnO by SrO additive were synthesized through a quick alkali mediated sol–gel method. The effect of adding ZnO and SrO on the bioactivity of cured ionomer cement was examined in simulated body fluid (SBF). Glass powder obtained in this way was used to prepare the GICs. The ideal powder: liquid (P:L) ratio determined to prepare the experimental GICs was equal to 1:1. The chemical process allows the development of glass powder at 400 °C which is the aim of the present paper. The powders were characterized by thermal analysis (TG/DSC), X-ray diffraction analysis (XRD), Fourier transforms infrared (FTIR) and Antibacterial influence. The results obtained showed that ZnO and SrO doping to glass ionomer cement block sites of the apatite nucleation led to retardation the apatite formation, high antimicrobial effect of samples against *Escherichia coli*, *Staphylococcus* Staph and also showed lack of water solubility by adding zinc contents.

**Keywords:** GICs, Sol-gel, Bioactivity, PPA, Antibacterials, Water sorption.

Conventional glass-ionomer cements (GIC) were first described by Wilson and kent in 1971 as materials consisting of a base—usually an ion-leachable, calcium aluminum fluorosilicate glass powder – that is combined with polyacrylic acid (PAA) or its copolymers <sup>(1)</sup>. Although GIC were introduced to dentistry in the 1970s, it was only from the early 1980s on that their physical properties were improved, thus making these materials more applicable and popular <sup>(2)</sup>. Several features have contributed to their wide acceptance, which include biocompatibility, good adhesion to dentin, ability to take up and release fluoride, minimal shrinkage on setting and resistance to degradation similar to that of dentin <sup>(3)</sup>. Solubility and water sorption is an important feature in assessing the clinical durability of dental cements. Consequently, solubility of dental cements has been widely evaluated both *in vitro* and *in vivo*<sup>(4)</sup>.

Glass polyalkenoate cements are materials made of calcium or strontium aluminofluorosilicate glass powder (base) combined with a water soluble polymer (acid). Kent called such materials “glass ionomer” cements, and that name has become part of the dental vernacular <sup>(5)</sup>. Glass ionomer cement components, when

mixed together, undergo a setting reaction involving neutralization of the acid groups by the powdered solid glass base. The curing reactions occur in two phases designated as gelation and maturation. These two cement-curing phases generate the GIC structure, a composite of cross-linked PAA reinforced with the reacted glass particles<sup>(6)</sup>. Without diminution of physical properties of the hardened cement, significant amounts of fluoride ions are released during this reaction.

The acid reacts with the basic SrO and ZnO to form a cross-linked metal polyacrylate salt containing residual SrO and ZnO particles. These Polyalkenoate cements set at body temperature without undergoing any polymerisation shrinkage and without significant evolution of heat<sup>(7)</sup>. Due to their excellent biocompatibility in the mouth, with no significant adverse reactions reported in over 20 years of use, attention was focused on the development of glass-ionomer cement<sup>(8)</sup>. Zinc is the second most prevalent trace element in the body and is required for proper cellular and immune function. The body needs zinc to metabolize carbohydrates, fats, proteins, alcohol and to dispose of carbon dioxide. Also, zinc is an essential trace element in the human body and has a stimulatory effect on bone formation. Human bone contains 0.0120–0.0250 wt% Zn, which is relatively high compared with the average Zn content of whole fat-free adult tissues (0.0030 Zn wt%) and that of plasma (0.78–1.0 Zn mg/L)<sup>(9,10)</sup>.

Sr - containing bioactive glasses in SiO<sub>2</sub>-CaO-SrO system by sol-gel method. The results pertaining to *in vitro* bioactivity analysis of the as developed glasses exhibited their strong potential towards osteoporosis treatment, dental applications and in bone tissue regeneration as well in bone remodeling. Further, substituting strontium ions in place of calcium, magnesium and to other alkaline earth cations showed good results in terms of bioactivity which sometimes claimed to be most challenging and also witnessed some phenomenal exchange of ideas and outcome which kindled the research of Sr-doped glasses with respect to the bone tissue engineering<sup>(11)</sup>.

Calcium fluoro-alumino-silicate glasses may be regarded as the basic type from which GICs are derived. These systems are prepared by the fusion method at temperatures ranging from 1200 to 1550 °C, depending on the composition. In this process, fluorine is lost from the melt. This fluorine loss is uncontrolled and results in variable composition between batches<sup>(12)</sup>.

Alternatively, soft chemistry has been used for synthesis of glasses because this route yields more homogeneous materials using lower processing temperatures than the conventional fusion method. Besides, the sol-gel process has the potential to yield glasses which cannot be otherwise prepared by the conventional melting method due to their high melting points<sup>(13)</sup>. Considerable efforts have been made to improve the properties of GICs using other types of glass powders derived from calcium fluoro-alumino-silicate systems with new components. The aim of this study, Zn containing glass ionomer cement was prepared by sol-gel method, with the purpose to analyse its bioactivity, water solubility, antibacterial properties and the influence of Zn, Sr and both of them on the deposition of HA on its surface.

### Materials and Methods

Tetraethyl orthosilicate (TEOS), calcium nitrate tetrahydrate Ca(NO<sub>3</sub>)<sub>2</sub>·H<sub>2</sub>O, sodium nitrate NaNO<sub>3</sub>, Aluminum nitrate Al(NO<sub>3</sub>)<sub>3</sub>·9H<sub>2</sub>O Zinc nitrate hexahydrate Zn(NO<sub>3</sub>)<sub>2</sub>·6H<sub>2</sub>O, Strontium nitrate Sr(NO<sub>3</sub>)<sub>2</sub>, Ammonium fluoride NH<sub>4</sub>F as source to fluorine and triethyl phosphate (TEP) (≥ 98%) were purchased from Fluka (Buchs, Switzerland). Ammonia solution, 33%, and nitric acid, 68%, were purchased from Merck, USA. Both nitric acid and ammonia solutions were diluted to 2 M using distilled water.

#### *Sol-gel synthesis of Zinc-doped glass ionomer*

Glass containing 0, 4, 6, 8 and 10 wt% of ZnO samples were synthesized through a quick alkali-mediated sol-gel technique<sup>(14)</sup>. ZnO was added to the glass compositions at the expense of SrO. Table 1 shows the nominal compositions and codes of the prepared bioactive glass, we make three solutions A), TEOS, distilled water and 2M nitric acid (as a hydrolysis catalyst), were successively mixed in ethanol and the mixture was left to react for 30 min under continuous magnetic stirring for the acid hydrolysis of TEOS. Then appropriate amounts of series reagents were added in the following sequence: (TEP), Ca(NO<sub>3</sub>)<sub>2</sub>·H<sub>2</sub>O, NaNO<sub>3</sub>, NH<sub>4</sub>F and Zn(NO<sub>3</sub>)<sub>2</sub>·6H<sub>2</sub>O, allowing 30 min for each reagent to react completely .B) Sr(NO<sub>3</sub>)<sub>2</sub> were mixed in the presence of distal water. C) Al(NO<sub>3</sub>)<sub>3</sub>·9H<sub>2</sub>O is mixed in distal water ,then solutions B&C are added on A by dropping for 30 min under continuous magnetic stirring. After the final addition, mixing was of all reagents continued for 60 min to complete hydrolysis. Ammonia solution of 2M concentration (a gelation catalyst) was dropped into the mixture. The mixture was then agitated with glass rod (like as mechanical stirrer) to prevent the formation of a bulk gel. Finally, each prepared gel was left to dry at 100-120°C for 2 days and sintered at 400°C for 2hr thermal oven.

**TABLE 1. Show Different additive of ZnO on the: SiO<sub>2</sub>-Al<sub>2</sub>O<sub>3</sub>-P<sub>2</sub>O<sub>5</sub>-CaO-Na<sub>2</sub>O-SrO-F<sup>-</sup>.**

Glass	Glass base							Additives
	SiO <sub>2</sub>	Al <sub>2</sub> O <sub>3</sub>	P <sub>2</sub> O <sub>5</sub>	CaO	Na <sub>2</sub> O	F <sup>-</sup>	SrO	ZnO
Zn <sub>0</sub> , Sr <sub>0</sub>	45	15	5	15	10	10	---	---
Zn <sub>0</sub>	45	15	5	10	5	10	10	---
Zn <sub>4</sub>	45	15	5	10	5	10	6	4
Zn <sub>6</sub>	45	15	5	10	5	10	4	6
Zn <sub>8</sub>	45	15	5	10	5	10	2	8
Zn <sub>10</sub>	45	15	5	10	5	10	0	10

### *Cement preparation*

The powder prepared by the sol–gel process was passed through a sieve with a mesh opening of 45 $\mu$ m, and then was used to produce the cement. The experimental GICs were prepared at room temperature by mixing the powder prepared by the sol–gel process with aqueous solutions 45–50% (m/m) of poly (acrylic acid) – PAA – MW 230,000. The specimens were made using a powder: liquid (P:L) ratio of 1:1. This P:L ratio (m/m) is in accordance with the manufacturer’s instructions<sup>(15)</sup>.

### *Characterization*

Thermogravimetric analyses (TGA), and differential calorimetric analyses (DSC) were performed for the dried gels using a computerized SETARAM labsys™ TG-DSC thermal analysis system. Scans were performed in the atmosphere, and in a temperature range of 50–1000 °C, at a rate of 10°C min<sup>-1</sup>. The materials were analyzed using aluminum oxide powder as a reference. The phase analysis of the samples was examined by X-ray diffractometer; model BRUKERaxs using Ni-filtered CuK $\alpha$  irradiation at 40 kV and 25 mA. The infrared spectra of the prepared glass were obtained using Fourier transform infrared spectrophotometer (FT-IR) (Model 580, Perkin-Elmer). Each sample used for infrared spectroscopic analysis was prepared according to KBr technique.

### *In-vitro assays in SBF*

In-vitro assays were performed in a simulated body fluid (SBF), proposed by Kokubo *et al.*<sup>(16)</sup>. The SBF solution has a composition and concentration similar to those inorganic parts of human plasma. During soaking process, each disc was soaked into 10 ml SBF contained in a polyethylene bottle. These bottles were covered with a tight lid and placed in thermodynamic incubator (shaking-water bath) at 37 °C for different time periods (control, 1, 4, 8 and 16 days). After being soaked, the discs were rinsed with deionized water and acetone and dried at room temperature.

### *Water solubility and water sorption assays in artificial saliva*

Degradation and water sorption assays were performed in artificial saliva, proposed by A. Preetha *et al.*<sup>(17)</sup>. The disks were placed in a glass vial containing 50 mL of artificial saliva, The vials were wrapped in aluminum foil to avoid light exposure and placed in an incubator at 37°C at intervals (1 D, 4 D and 8 Days) removed, blot-dried, weighed, and then returned to water. This was continued until a constant weight was achieved ( $W_1$ ). The discs were removed from the water and replaced in a desiccator containing calcium sulfate, at 37°C and were reweighed until a constant weight had been achieved. It was subsequently dried by placing it into desiccator at 80°C for 1 hr and then reweighed for the last time ( $W_2$ ). These steps were carried out to evaluate sorption (A) and solubility (S) according to Oysaed & Ruyter<sup>(18)</sup> formula:  $A = W_2 - W_1/V$  and  $S = W_1 - W_3/V$ , where:  $W_1$  is the sample weight before immersion,  $W_2$  is the sample weight after

immersion, and  $W_3$  is the sample weight after immersion and desiccation, and  $V$  is the sample volume. Finally, the results were analyzed by means of one-way ANOVA statistical program.

#### *Antibacterial tests*

Antibacterial property was examined by mixing the same physiologic solution was used for bacteria. 500 $\mu\text{L}$  of containing bacteria solution were in contact in plate at room temperature for 15, 30 min , 1 and 2hr , After each sampling time, EC X-GLUC agar for *E. coil* and AZIDE MALTOSE agar (KF) for *S. Stph* were added to sample plates . The plates were aerobically incubated 48hr at 37 $^{\circ}\text{C}$  for *E. coil* , *S. Staph* . The number of the colonies was counted.

### **Results and Discussion**

#### *Thermal analysis*

Thermogravimetric analysis (TGA) and differential scanning calorimetric (DSC), analysis curves for sample ( $\text{Zn}_4$ ) are shown in Fig. 1,2. The TGA curves of all samples showed three main stages of weight losses as the heating process proceeded from room temperature up to 800  $^{\circ}\text{C}$ . Those weight losses appeared at the temperature intervals of 30-160,160–224, 224–305, and 305–700  $^{\circ}\text{C}$  for all samples. The first weight loss was attributed to the removal of water which appears as (humidity and physically adsorbed water) from the surface and any the residual alcohol in the pores of the dried gel<sup>(19)</sup>. This stage was reflected in the DCS curves of sample ( $\text{Zn}_4$ ) as the first large endothermic peak centered at about 160 $^{\circ}\text{C}$ <sup>(19)</sup>, as shown in Fig. 1. The second weight loss was reflected in the exothermic peaks centered around at 224 $^{\circ}\text{C}$  on the DSC curve of sample ( $\text{Zn}_4$ ), which is most likely due to first crystallization temperature for  $\text{CaF}_2$  phase separation. The third weight loss occurred from the end of the second drop in mass around at 284 $^{\circ}\text{C}$  until around at 551 $^{\circ}\text{C}$  leading to an apparent weight loss about 13.45 % of the total weight loss. This weight loss is due to second crystallization temperature for calcium aluminium silicate ( $\text{Ca}_3\text{Al}_6\text{Si}_2\text{O}_{16}$ ), as confirmed by the corresponding second exothermic peak at 700  $^{\circ}\text{C}$  in the DSC trace<sup>(20)</sup>.

#### *X-ray diffraction analysis*

The powder prepared at 400  $^{\circ}\text{C}$  by the sol–gel process was analyzed by X-ray powder diffraction (XRD) to identify the crystal phases. In Fig. 3, four peaks at  $2\theta$  values of 28.27 $^{\circ}$ , 47.09 $^{\circ}$ , 55.7 $^{\circ}$  and 68.66 $^{\circ}$  were observed. This crystalline phase corresponds to the standard JCPDS file no. (88-2301), which refers to the presence of fluorite ( $\text{CaF}_2$ ) phase. The crystallization of  $\text{CaF}_2$  occurs because  $\text{Ca}^{2+}$  and  $\text{F}^-$  ions are relatively mobile in network<sup>(12)</sup>.

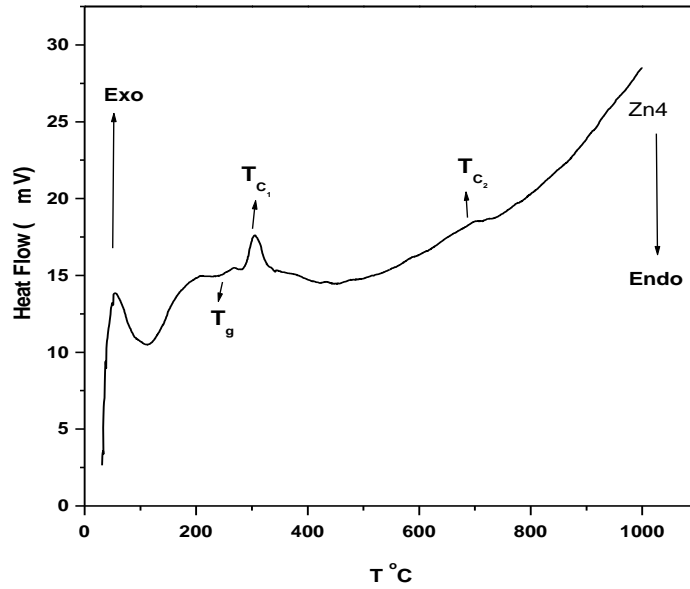


Fig. 1. DSC curves of sol-gel glass after drying for all samples at 80°C and 120°C for 2 days.

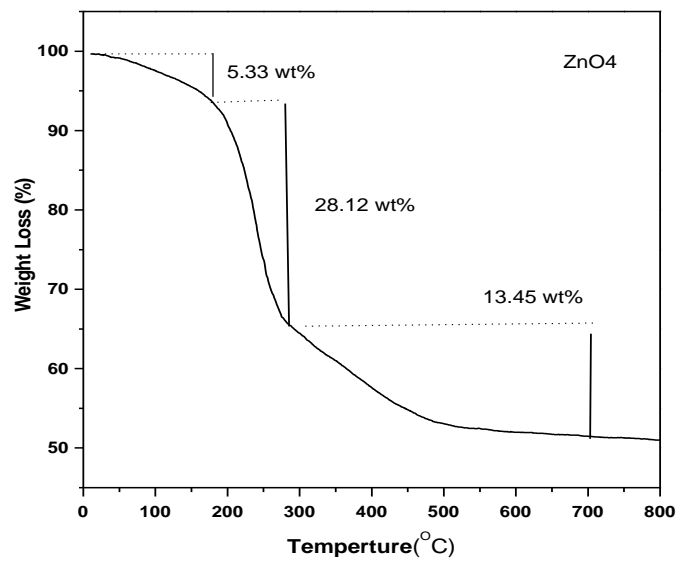
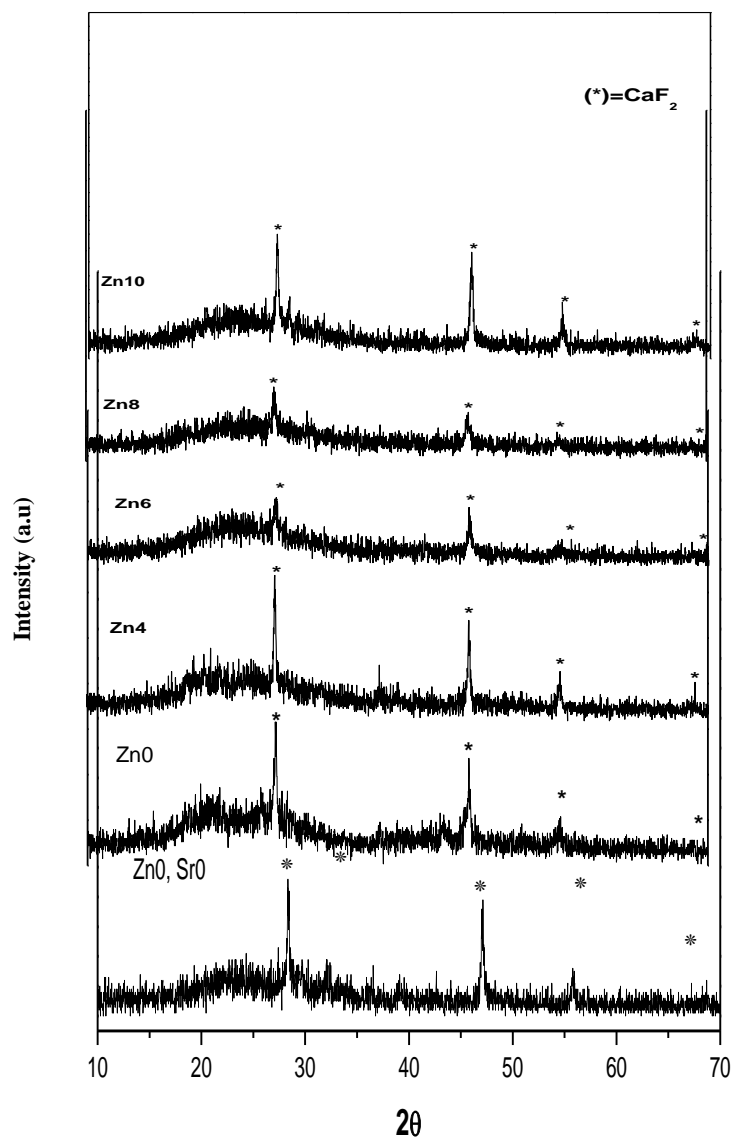


Fig. 2. TGA curve of sol-gel glass for Zn4 sample.



**Fig.3. XRD Pattern of all sol-gel GIC samples soaking in SBF.**

The XRD analysis results of annealing gel glass ionomer cement samples after soaking in SBF for  $\text{Zn}_0$ ,  $\text{Zn}_4$  and  $\text{Zn}_{10}$  at  $400^\circ\text{C}$  are shown in Fig. 4. After soaking in SBF for 16 days, there are two phases formed on the GICs surface.

The first phase is poor-crystallized HA layer exhibit as small peaks which overlapping with  $\text{CaF}_2$  peaks. In addition, the second phase is the well-crystallized phase calcium Oxide ( $\text{CaO}$ ).

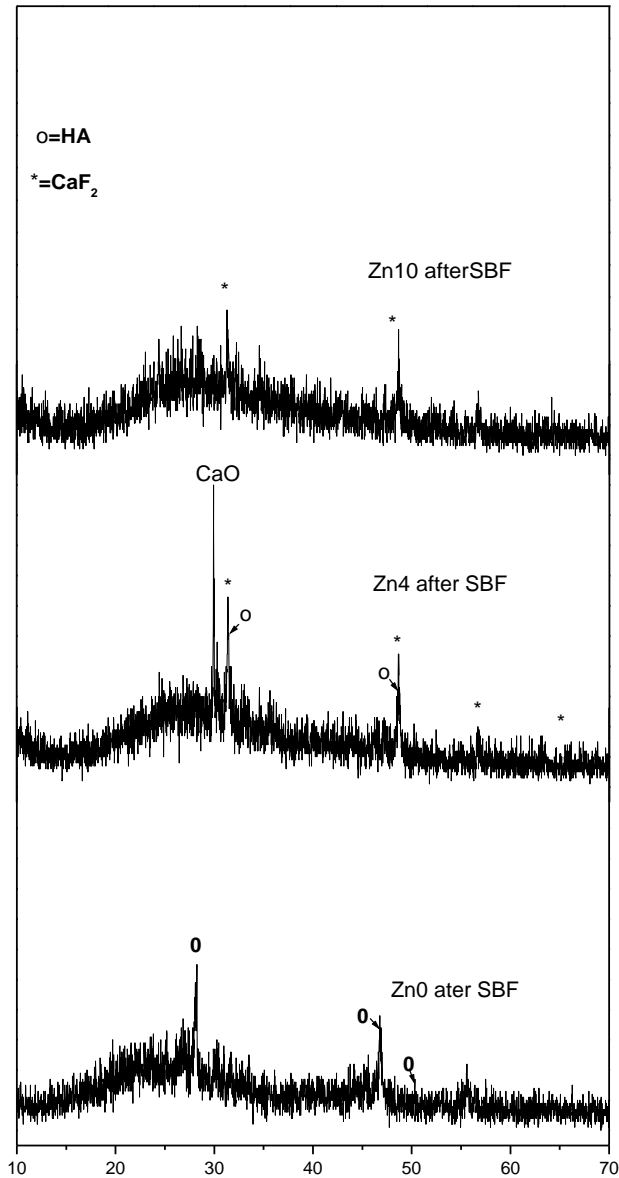


**Fig. 4.** XRD Pattern of all sol-gel GIC samples after soaking in SBF.

Generally, the increase in the intensity and decrease in the width of the apatite peaks of all samples in SBF depends on amount of ZnO contents. Therefore, the presence of Zn<sup>2+</sup> ions in the GICs composition causes inhibition or retardation of calcium phosphate precipitation layer by adsorbing onto the top and block sites of the calcium phosphate nucleation<sup>(21)</sup>.

#### FTIR analysis

The FTIR spectra of the cement samples (cured for 24 hr) were used to characterize their curing reactions and chemical structure of silicate network for all samples as shown in Fig.5. The observed bands of all samples are listed in Table 2. For all samples before adding PAA, the bands in the range of 1000–1300 cm<sup>-1</sup> correspond to the Si–O–Si asymmetric stretching vibration whereas the band located at ~ 440-540 cm<sup>-1</sup> corresponds to the vibrational mode of the bending of Si–O–Si<sup>(22)</sup>. The two absorption bands located at ~ 670-740 cm<sup>-1</sup> corresponds to Si–O symmetric stretch of bridging oxygen (BO) between tetrahedron chains.

**TABLE 2. Assignments of Infra-red absorption bands of Zn<sub>0</sub>, Zn<sub>4</sub>, Zn<sub>6</sub>, Zn<sub>8</sub> and Zn<sub>10</sub>.**

Band range cm <sup>-1</sup>	Zn <sub>0</sub>	Zn <sub>4</sub>	Zn <sub>6</sub>	Zn <sub>8</sub>	Zn <sub>10</sub>
Si-O-Si (b) 540 - 440	440	441	440	442	443
Si-O (s) 670 – 740	.....	680	731,740	687	690
Si-O-Si (s) 1000 - 1300	1113	1095	1089	1085	1078
P-O (b) 550 - 640	607	570	566	562	555
C-O (s) 1300 - 1500	1461	1462	1520	1460	1464
H-O-H 1630 - 1650	1644	1632	1650	1640	149
H-O-H (s) 3350 - 3600	3350	3438	3453	3432	3430
NO <sub>3</sub> <sup>-</sup> 1385	1385	1384	1386	1382	1385

On the other hand, FTIR spectra of glass after adding with PAA (GICs) are shown in Fig. 6. The general features observed were a progressive conversion of

acid  $-\text{COOH}$  groups to salt  $-\text{COO}^-$  groups as metal salts were formed. On neutralization of organic acid the main characteristic is loss of bands around  $1250$  and  $1710\text{ cm}^{-1}$  assigned to C-O and C=O stretch of poly(acrylic acid) in the FTIR spectra. Loss of these bands is due to formation of polyacrylate salts<sup>(23,24)</sup>.

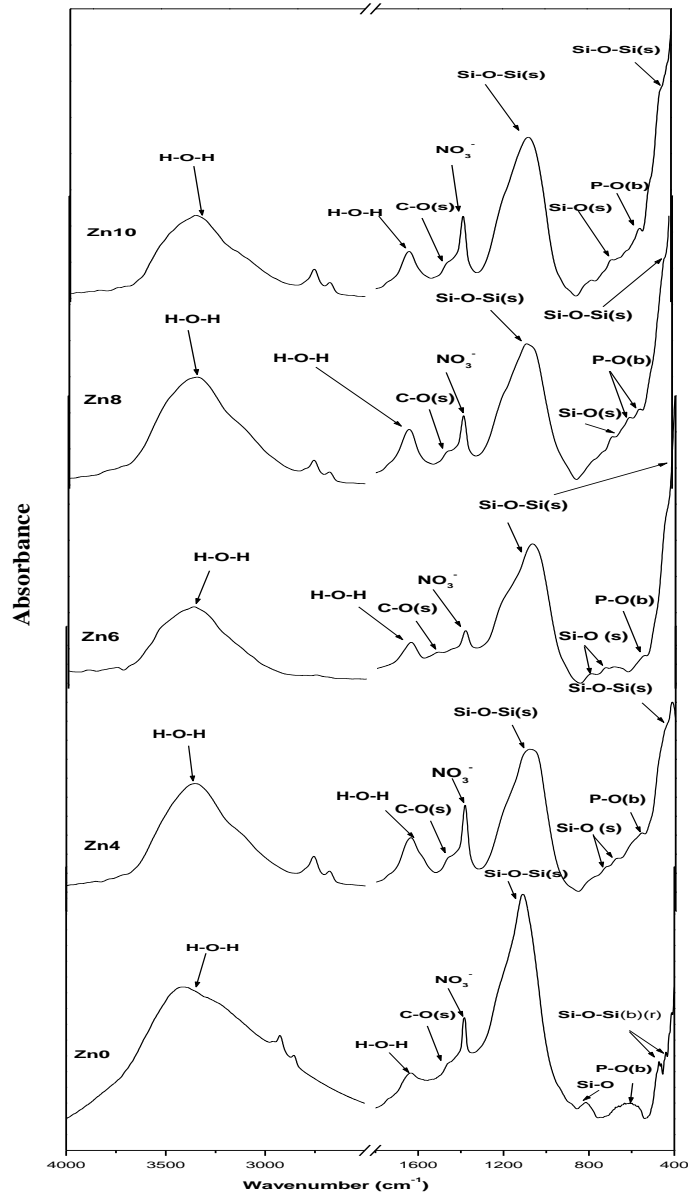
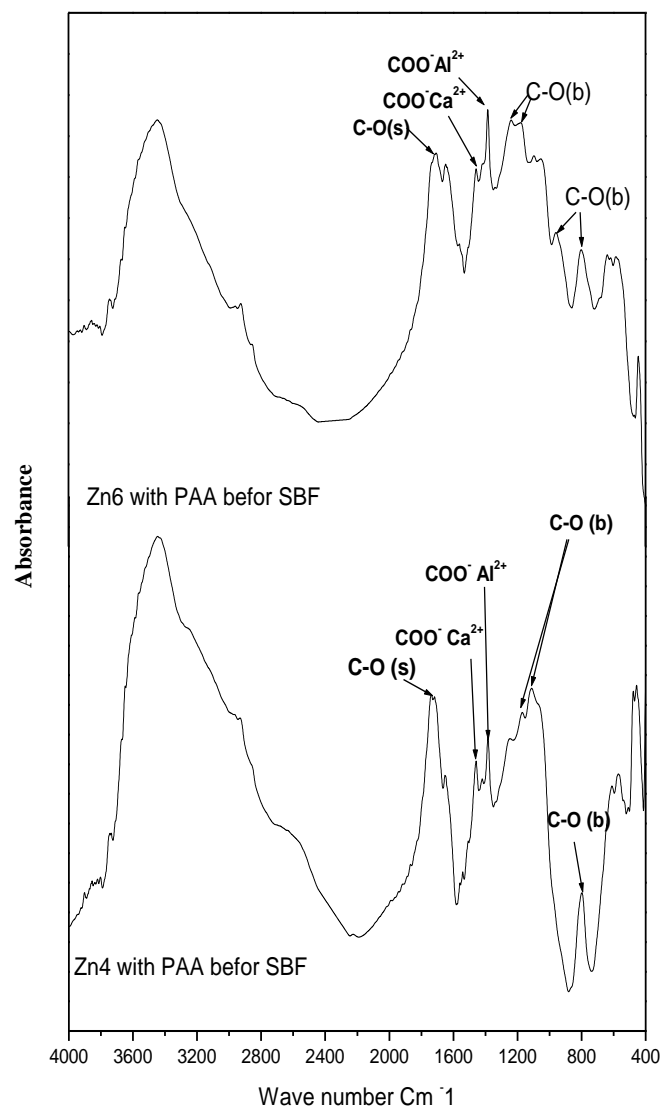


Fig. 5. FTIR spectra of  $\text{Zn}_0$ ,  $\text{Zn}_4$ ,  $\text{Zn}_6$ ,  $\text{Zn}_8$  and  $\text{Zn}_{10}$  sol-gel glass.



**Fig. 6. FTIR spectra of  $\text{Zn}_4$  and  $\text{Zn}_6$  sol-gel GICs after mixing with poly(acrylic acid) before SBF.**

As can be seen in Fig. 6 the bands observed around  $1700 \text{ cm}^{-1}$  were substituted progressively and other bands can be observed in the spectra. These bands around  $1460$  and  $1640 \text{ cm}^{-1}$  (after 24 hr) could be assigned to symmetric and asymmetric  $\text{COO}^-$  stretch of aluminum polyacrylate salt and the bands

around  $1380\text{cm}^{-1}$  assigned to symmetric  $\text{COO}^-$  stretch of calcium poly acrylate. These data confirm that the reaction between the particles of the powder and poly(acrylic acid) solution was completed within 24hr after that cement had been prepared<sup>(15)</sup>

Figure 7 shows FTIR absorption spectra of glass ionomer cement samples after soaking in SBF for 16 days. These spectra of GICs sample after SBF immersion showed either a single peak or a split peak approximately at  $610\text{ cm}^{-1}$  and  $530\text{ cm}^{-1}$  which attributed to P–O bending vibration<sup>(25)</sup>. This is the most characteristic region for apatite and other phosphates, and it corresponds to P–O bonding vibrations in a  $\text{PO}_3^{4-}$  tetrahedron and indicates the presence of crystalline calcium phosphates including apatite phase (HA), but with small amount. This delay in apatite layer formation is due to two reasons: The first is the presence of  $\text{Zn}^{2+}$  ions which blocking the nucleation site of apatite phase.

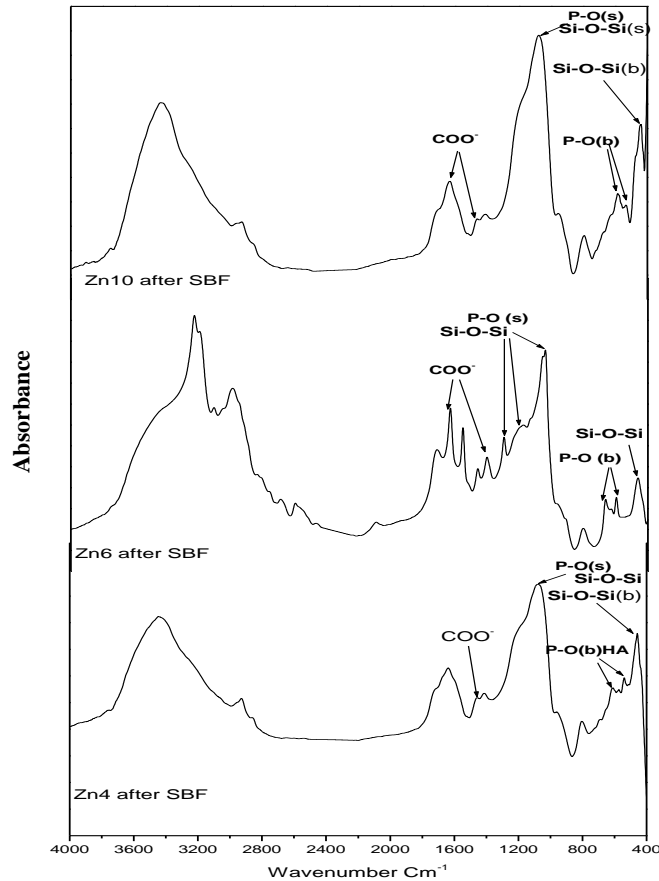


**Fig. 7.** FTIR spectra of  $\text{Zn}_4$ ,  $\text{Zn}_6$  and  $\text{Zn}_{10}$  sol-gel GICs after mixing with poly(acrylic acid) and soaking in SBF.

The second is the presence of PAA, which plays a role in the change of pH value in SBF solution<sup>(26)</sup>. Consequently, it is assumed that PAA does not inhibit the formation of the apatite nucleation sites, but does inhibit the formation of apatite and/or crystal growth on these nucleation sites<sup>(27)</sup>. Therefore, the apatite formation on the surface of the glass ionomer cement may be inhibited by the adsorption of PAA and release of Zn ions to compete with Ca ions in SBF solution.

#### *Water solubility and water sorption analysis*

The water sorption and solubility of dental restorative materials are of considerable clinical importance and cannot be neglected<sup>(28)</sup>. According to Tae Hyung Kim *et al.*<sup>(29)</sup>, high strength and low solubility are desirable for any base or lining material. The powder and liquid of glass ionomers were weighed and, after mixing, the materials were inserted into the teflon mould with a stainless steel spatula. The moulds (4 mm in diameter and 6 mm in height). A piece of film was placed onto the material in the mould and covered with a glass slide. Hand pressure was applied for 20 seconds while excess material was extruded from the top of the mould. The specimens were recommended exposure time through a glass plate. The water sorption measurements actually measured the net gain in weight of a specimen as a result of the ingress of water molecules and egress of monomers and other small molecules<sup>(30)</sup>.

Figures 8 and 9 show water sorption and solubility of SrOZnO, ZnO, Zn10 samples after soaking in artificial saliva. As can be seen that, cement without strontium and zinc contents show the highest value of water sorption and water solubility followed by strontium GIC, while cement containing zinc shows the lowest values of the three materials tested regarding both water sorption and water solubility as shown in Fig. 8 and Fig. 9.

This due to, the ionic radius of  $\text{Zn}^{2+}$  (0.74Å) is smaller than the ionic radius of  $\text{Sr}^{2+}$  (1.18Å). So, the addition of ZnO has a smaller disrupting effect on the structure and hence it will strengthen the network<sup>(31)</sup>. This result was in agreement with that of Boyd *et al.*<sup>(32)</sup> who worked on a SrO–CaO–ZnO– $\text{SiO}_2$  glass ionomer composition and that of Abou Neel *et al.*<sup>(33)</sup> who worked on Sr-doped phosphate glasses.

The replacement may cause a significant decrease in GIC solubility due to decreasing the network disorder caused by smaller ionic radius of Zn compared with Sr. The decreased disorder can cause decrease in glass solubility and water sorption, because solubility is a trade-off between the energy required to dissociate the structure and the energy released upon hydration of the resultant ions. Therefore, it seems reasonable to suggest that a more ordered network produces a more stable (or more soluble) structure.

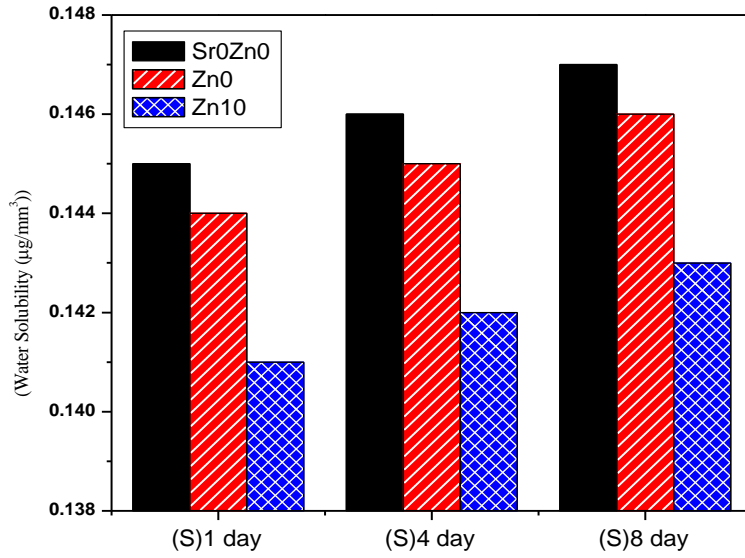


Fig. 8. Bar chart showing water solubility in  $\mu\text{g}/\text{mm}^3$ .

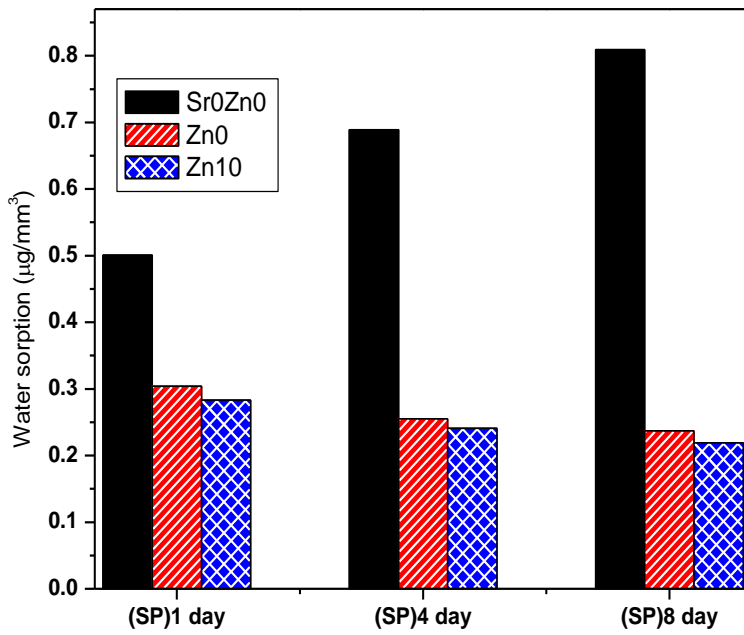


Fig. 9. Bar chart showing water sorption in  $\mu\text{g}/\text{mm}^3$ .

*Antibacterial test of (GICs)*

Plates (A, B) illustrate the test results for the glass ionomer cement containing zinc, respectively. The diameters of the halo zone for the antibacterial materials are demonstrated in Table 3. The diameters of haloes of inhibition were measured using calipers. Disc diameters were measured at the same point and the size of inhibition zones was calculated as follows: Size of inhibition zone (mm) = (diameter of zone of inhibition – diameter of disc) × 1/2, as shown in Fig. 10.

**TABLE 3. The diameter of the halo zone which made by the antibacterial materials.**

Sample Name	Size of inhibition zone area (cm)	
	<i>Escherichia coli</i>	<i>Staphylococcus Staph</i>
Zn <sub>0</sub> ,Sr <sub>0</sub>	0.30cm	0.35cm
Zn <sub>0</sub>	0.35cm	0.70cm
Zn <sub>4</sub>	0.40cm	0.75cm
Zn <sub>6</sub>	0.44cm	0.80cm
Zn <sub>8</sub>	0.50cm	0.85cm
Zn <sub>10</sub>	0.67cm	1.0cm

The antibacterial assay revealed that samples Zn<sub>0</sub>, Zn<sub>4</sub>, Zn<sub>6</sub>, Zn<sub>8</sub> and Zn<sub>10</sub> had an antibacterial effect against *Staphylococcus Staph* and *E. coli* as shown in Fig.(10). There is a clear difference between the inhibitory effects of the cements on *E. coli* and *S. Staph viscosus*. Figure 10 illustrates the inhibition zones around the GICs disks in the agar plate after 48 hr. The diameters of inhibition zones formed around all GICs disks were about 0.35-67 cm to *E. coli* and 0.7-1 cm to *S. Staph*.

The antibacterial action of the Zinc-doped GICs was attributed to the leaching out of Zn<sup>2+</sup> ions from the glass matrix. Phan *et al.*<sup>(34)</sup> studied the antibacterial effect of Zn<sup>2+</sup> ions and suggested that zinc inhibits multiple activities in the bacterial cell, such as glycolysis, transmembrane proton translocation and acid tolerance, it has been shown to exhibit an antibacterial effect at considerably lower concentrations than many antimicrobial agents<sup>(35)</sup>. Nevertheless, the cements without Sr and with different Zn content exhibited different inhibition of both bacterial species.



**Fig. 10.** The antifungal efficiency of antibacterial glass ionomer cement containing zinc in the test microorganisms (A: *Escherichia coli* , B: *Staphylococcus Staph*).

### Conclusion

Zinc containing and zinc, strontium free GICs were successfully prepared by quick alkali mediated sol-gel method. Present results indicate that, with the partial substitution of ZnO for SrO in glass composition and then mixed with PPA, the formation of apatite-like layer is delayed, confirming that, not all GICs surfaces are equally active for nucleation of apatite crystals. Therefore, the apatite formation on the surface of the GICs may be inhibited by the adsorption of PAA and release of Zn ions to compete with Ca ions in SBF solution. The solubility of dental cements influences both their rate of degradation and their biological compatibility. Because of this, the water sorption and solubility of dental cements are of considerable clinical importance and cannot be overlooked. The antibacterial assay revealed that all GICs samples had an antibacterial effect against different type of bacteria, which could demonstrate their ability to treat bone infection and has been recognized as an antibacterial agent. Finally, GIC should be characterized as three properties, the first is formation of a small apatite layer to biocompatible with the jaw bone, the second is antibacterial effect to resist oral bacteria and the third is low degradation, to resist artificial saliva which is the most important feature.

### References

1. **Wilson, A.D. and Kent, B.E.**, *J. Appl. Chem. Biotechnol.* **21**, 313(1971) .
2. **Abdalla, Al. and Garcia-Godoy, F.**, Bond strengths of resin-modified glass-ionomers and polyacid-modified resin composites to dentin. *Am. J. Dent.* **10**, 291-294 (1997).
3. **Fruits, T.J, Coury, T.L., Miranda, F.J. and Duncanson, M.G. Jr.**, Uses and properties of current glass-ionomer cements: a review. *Gen. Dent.*, **44**, 410-418 (1996).
4. **Yoruc, H.A.B. and Karaaslan, A.**, Effect of water storage on the mechanical properties of zincpoly carboxylate cements. *Digest J. of Nanomaterials and Biostructures*, **2**(2), 243-52 (2007).
5. **Wilson, A.D. and McLean, J.W.**, “*Glass Ionomer Cement* ”. Chicago: Quintessence Publishing Co; 14 (1988).
6. **Pires, R.A., Fernandez, C., Nunes, T.G. and Mater, J.**, *Sci. Mater. Med.* **18** , 787-796 (2007).
7. **Smith, D.C.**, Development of glass-ionomer systems, *Biomaterials*, **19**, 467 (1998).
8. **Mount, G.J.**, Clinical performance of glass-ionomers, *Biomaterials*, **19**, 573 (1998).
9. **Underwood, E.J.**, “*Trace Element in Human and Animal Nutrition*”, 4<sup>th</sup> ed., p. 196, Academic Press, London (1997).
10. **Yamaguchi, M., Yamaguchi, R. and Suketa, Y.**, Stimulatory effect of zinc on bone formation in tissue culture. *Biochem. Pharmacol.* **35**(5), 773-777 (1987) .

11. **Lao, J., Nedelec, J.M. and Jallot, E.,** New strontium-based bioactive glasses: Physicochemical reactivity and delivering capability of biologically active dissolution product. *J. Mat. Chem.* **19**, 2940-2949 (2009).
12. **Wood, D. and Hill, R.** Glass ceramic approach to controlling the properties of a glass ionomer bone cement. *Biomaterials*, **12**,164–70 (1991).
13. **Taira, M. and Yamaki, M.,** Preparation of SiO<sub>2</sub>–Al<sub>2</sub>O<sub>3</sub> glass powders by the sol–gel process for dental applications. *J. Mater Sci. Mater Med.* **6**,197–200 (1995).
14. **El-Gohary, M.I., Tohamy, Kh. M., El-Okr, M.M. Ali, A.F. and Soliman, E.,** Influence of composition on the *in-vitro* bioactivity of bioglass prepared by a quick alkaline –mediated sol- gel method, *Nature and Science*, **11**(3), 26-33 (2013).
15. **Zaghetea, M.J.B.M.A., Gimenes, R. and Padovani, G.C.,** Determination of the properties of an experimental glass polyalkenoate cement prepared from niobium silicate powder containing fluoride. *Dental Materials*, **24** ,124-128 (2008).
16. **Kokubo, T. and Takadama, H.,** How useful is SBF in predicting *in vivo* bone bioactivity. *Biomaterials*,**27**, 2907–2915 (2006).
17. **Preetha, A. and Banerjee, R.,** Comparison of artificial saliva substitutes. *Artif. Organs*, **18**, (2), (2005)
18. **Oysaed, H. and Ruyter, I.E.,**Water sorption and filler characteristics of composites for use in posterior teeth. *J. Dent Res.* **65**,1315–1318 (1986).
19. **Oki, A., Parveen, B., Hossain, S., Adeniji, S. and Donahue, H.,** *J. Biomed. Mater. Res.* **69**, 216-21 (2004).
20. **Jonesa, J.R., Ehrenfried, L. M. and Hench, L.L.,** *Biomater.* **27**, 964-973 (2006).
21. **Hesaraki, S., Alizadeh, M. and Nazarian, H.,** Physico-chemical and *in vitro* biological evaluation of strontium/calcium silicophosphate glass. *Journal of Materials Science: Materials in Medicine*, **21**, 695-705 (2010).
22. **Aguiar, H. Serra, J., González, P. and León, B.,** *J. Non-Cryst.Solids*, **355**, 475-480 (2009).
23. **Young, A.M.,** FTIR investigation of polymerisation and polyacid neutralization kinetics in resin-modified glass-ionomer dental cements. *Biomaterials* **23**, 3289–95 (2002).
24. **Young, A.M., Sherpa, A., Pearson, G., Schottlander, B. and Waters, D.N.,** Use of Raman spectroscopy in the characterisation of the acid–base reaction in glass-ionomer cements. *Biomaterials*, **21**, 1971–9 (2000).
25. **Vidueau, V. and Dupius, J.J.,** Phosphates and biomaterials. *Eur. J. Solid State Inorg. Chem.* **28**, 303–343 (1991).
26. **Kamitakahara, M., Kawashita, M., Kokubo, T. and Nakamura, T.,** Effect of polyacrylic acid on the apatite formation of a bioactive ceramic in a simulated body *Egypt. J. Biophys. Biomed. Engng.* **Vol. 13** (2012)

- fluid: Fundamental examination of the possibility of obtaining bioactive glass-ionomer cements for orthopedics use. *Biomaterials*, **22**, 3191-3196 (2001).
27. **Amjad, Z.** Performance of polymeric additives as hydroxyapatite crystal growth inhibitors". *Phosphorus Res. Bull.* **5**, 1-12 (1995).
  28. **Keyf, F., Tuna, S.H., Sen, M. and Safrany, A.,** Water sorption and solubility of different luting and restorative dental cement. *Turk. J. Med. Sci.* **36** (1), 47-55 (2006).
  29. **Kim, Tae Hyung, Jivraj, Sajid A. and Donovan, Terry E.,** Selection of Luting Agents: Part 2. *Californian Dental Association Journal*, **34** (2), 161-66 (2006).
  30. **Chai, J., Takahashi, Y., Hisama, K. and Shimizu, H.,** Water sorption and dimensional stability of three glass fiber reinforced composites. *Int J. Prosthodont*, **17**, 195-9 (2004).
  31. **Knowles, J.C., Franks, K. and Abrahams, I.,** *Biomaterials*, **22**, 3091 (2001).
  32. **Boyd, D., Towler, M.R., Watts, S., Hill, R.G., Wren, A.M. and Clarkin, O.M.,** *J. Mater. Sci. Mater. Med.* **19**, 953 (2008).
  33. **Abou Neel, E.A., Chrzanowski, W., Pickup, D.M., O'Dell, L.A. Mordan, N.J., Newport, R.J., Smith, M.E. and Knowles, J.C.,** *J. R. Soc. Interface*, **6**, 435 (2009).
  34. **Phan, T.N., Buckner, T., Sheng, J., Baldeck, J.D. and Marquis, R.E.,** *Oral Microbiol. Immunol.* **19**, 31 (2002).
  35. **Brading, M.G., Cromwell, V.J., Jones, N.M., Baldeck, J.D. and Marquis, R.E.,** *Int. Dent. J.* **53**, 363 (2003).

(Received 18 / 2 /2014;  
accepted 25 / 3/ 2014)

## تحضير الزجاج الايوني المتمائل (الأسمنتي) في نظام $\text{SiO}_2$ , $\text{Al}_2\text{O}_3$ , $\text{Na}_2\text{O}$ , $\text{CaO}$ , $\text{P}_2\text{O}_5$ , $\text{F}^-$ وبإضافة أكسيد الزنك بدلاً من أكسيد الاسترانثيوم باستخدام طريقة السول - جيل

خيري محمد تهلمى عريبة ، ناجى عبد السميع\* طه محمد طعيمة\*\* وإسلام سليمان  
قسم الفيزياء كلية العلوم (بنين)- جامعة الازهر- القاهرة\* قسم المواد الحيويه بكلية  
طب الأسنان و\*\*مركز المعرفة بكلية الصيدلة جامعة مصر للعلوم والتكنولوجيا  
مدينة ٦ أكتوبر - مصر .

تم تحضير الزجاج الأيوني الأحادي (الأسمنتي) في نظام  $\text{SiO}_2$ ,  $\text{Al}_2\text{O}_3$ ,  $\text{Na}_2\text{O}$ ,  $\text{CaO}$ ,  $\text{P}_2\text{O}_5$ ,  $\text{F}^-$  وبإضافة أكسيد الزنك بدلاً من أكسيد الاسترانثيوم وذلك باستخدام طريقة السول - جيل. إن تأثير إضافة أكسيد الزنك وأكسيد الاسترانثيوم على النشاط الحيوي للزجاج الأحادي المتمائل قد تم غمره في الوسط المشابه لبلازما دم الانسان (SBF). وتم أيضاً استخدام المسحوق الزجاجي الذي تم الحصول عليه بهذه الطريقة في تحضير الزجاج الأسمنتي. وتتألف التركيبة من النسب التالية: نسبة (البوليمر : المسحوق) (١:١). وقد تم تحضير العينة المذكورة في البحث عند ٤٠٠ م° ، وهذا هو الهدف من البحث. وقد تم توضيح خصائص العينات المحضرة باستخدام طريقة التحليل التفاضلي الحرارى (TG/DSC) واستخدام حيود الأشعة السينية (XRD) وطريقة فورييه باستخدام الأشعة تحت الحمراء (FTIR) وتأثير هذه العينات المضاد علي البكتريا. وعند إضافة أكسيد الزنك وثاني أكسيد الاسترانثيوم إلى الزجاج الأسمنتي أدى إلى عدم تكوّن طبقة الأباتيت (apatite) بمعدل عالي. وتم أيضاً إيضاح أن عنصرى الزنك والاسترانثيوم لهما تأثير على عدم نمو البكتريا ، وخاصة على بكتريا (*E-coli*) وستافيلوكوكس *Staphylococcus Staph*. وعند اضافة عنصر الزنك الى العينات المحضرة قلّة نسبة ذوبانها في الماء.

